LABORATORY OF PLASMA STUDIES

Observations of the Thermalization of the Neutralizing Electrons in Intense Ion Beams

R. Kraft* and B. R. Kusse

Laboratory of Plasma Studies
Cornell University
Ithaca, N.Y. 14853

LPS 359 July 1986

CORNELL UNIVERSITY

ITHACA, NEW YORK

Observations of the Thermalization of the Neutralizing Electrons in Intense Ion Beams

R. Kraft* and B. R. Kusse

Laboratory of Plasma Studies
Cornell University
Ithaca, N.Y. 14853

LPS 359 July 1986

OBSERVATIONS OF THE THERMALIZATION OF THE NEUTRALIZING ELECTRONS IN INTENSE ION BEAMS

R. Kraft* and B. R. Kusse
Laboratory of Plasma Studies and
School of Applied and Engineering Physics
Cornell University, Ithaca, New York

Abstract

Vacuum propagation of intense, pulsed ion beams relies on the existence of charge and current neutralization by electrons drawn into the beam channel by the electrostatic forces of the ions. We report here a set of measurements of the temperature of the neutralizing electrons and of the beam potential which support existing theories of the time and spatial development of the neutralizing space charge and current.

Research supported by Office of Naval Research Contract 0014-82-K-2059

*present address: AVCO Research Laboratory, Everett, MASS.

Introduction

The propagation of intense pulsed ion beams is crucially dependent on countering the space charge effects of the beam ions. This means there must be a source of electrons for the propagating channel. These electrons can come from plasma existing in the channel itself or, in the case of vacuum propagation, from an external electron source such as the cathode plasma or a grounded conductor that can be turned on by some of the energetic ions.

The propagation and many of the properties of the ion beams of interest to this paper have been summarized in two review articles (1), (2). The beam source (Figures 1 and 2) used for the measurements discussed below was a magnetically insulated, field inclusion or race track diode (2) and produced an 80 nanosecond fwhm, 360 keV, 10 kA, 65 amp/cm^2 proton beam (two beam pulses were generated due to a mismatch between the ion diode and the transmission line). The measured ion beam divergence (biased charge collectors) and net beam current (Rogowski loops) indicated that the beam was charge and current neutralized. A mechanism for vacuum neutralization of this beam by the cathode plasma electrons has been proposed (3), (4), (5), and is briefly summarized below.

While the neutralized, propagating state of ion beams is routinely observed, no experimental verification of the mechanism by which the beam arrives at this state has been reported. In this paper we present the first observations of the spatially resolved beam potential and electron velocity distribution which confirm these earlier pictures of the neutralization process.

Theory of Neutralization

A mechanism for vacuum neutralization of intense pulsed ion beams was first proposed by Humphries (3). In his model, the electrostatic forces of the cold ion beam emerging from the cathode plasma draw electrons from this plasma into the propagation channel. The electrons are accelerated through a sheath region to a velocity equal to twice the ion drift speed. The sheath thickness is equal to,

$$x_s \equiv 4\left[\frac{1}{2}\frac{\epsilon_o m_e v_i^2}{n_i e^2}\right]^{1/2} \qquad (1)$$

$$x_s \approx 0.2\ cm. \quad (\textit{typical experimental value})$$

where v_i and n_i are the ion beam velocity and density and m_e and e are the mass and charge of the electron. When these $2v_i$ electrons reach and overshoot the head of the ion beam they are decelerated to zero velocity. The density of the zero velocity electrons is equal to the density of the $2v_i$ electrons which is one half the ion density. This results in complete current and space charge neutralization of the ion beam.

When the ion emission from the diode terminates, the ion beam disconnects from the cathode. As the end of the ion beam passes over the zero velocity electrons in the beam channel these electrons are accelerated back up to $2v_i$. The electron acceleration and deceleration occur in sheath regions at the end and front of the ion beam. The potential drop across the sheath regions is given by,

$$\Phi_b = \frac{1}{2}\frac{m_e\, 4\, v_i^2}{e} << \frac{1}{2}\frac{m_i v_i^2}{e} \qquad (2)$$

where m_i is the ion mass. This potential is able to perpetuate the electron distribution with negligible effect to the ions and the beam can propagate in this space charge and current neutralized state. This situation is depicted in Figure 3. where the electron and ion distributions have been ideally described with delta functions.

While the two delta function electron distribution provides the required space charge and current neutralization and is self consistent with the beam potential Φ_b, the distribution is clearly unstable. There is a strong convective two-stream instability between the zero and $2v_i$ electrons.

This thermalization process has been investigated analytically and computationally (4), (5) with the results predicting that the electron distribution becomes thermalized with an average velocity v_i and a thermal spread of approximately v_i (Figure 4.). Computer simulations (4) predict that some of the electrons are accelerated to over $2v_i$ within a distance of approximately x_s from the cathode and the thermalization occurs over a distance of approximately $10\, x_s$. The beam potential was predicted to drop from an initial value of approximately,

$$\frac{1}{2}\frac{m_e(2.6\, v_i)^2}{e} \qquad (3)$$

near the cathode to a value of approximately,

$$\frac{1}{2}\frac{m_e(v_i)^2}{e} \qquad (4)$$

when the electrons have thermalized. It was the intent of the experiments described in this paper to observe some of these neutralization and thermalization phenomena.

Diagnostics

Two diagnostic techniques were employed, one to measure the neutralizing electron velocity distribution function (biased charge collector) and the second to measure the beam floating potential (capacitive probe). The electron velocity distribution was found by measuring the net current collected by a charge collector as a function of the bias voltage ($0 \leq V_o \leq 1500$ volts). The data was fitted to curves generated by a self-consistent biased charge collector analysis (6), (7) which takes into account ion and electron space charge in the collector. In this model the potential required to maintain charge neutrality in the charge collector was calculated as a function of bias voltage. For the parameters encountered in the experiment, the potential inside the charge collector was found to be between the aperature and collector plate potentials when the bias voltage was greater than approximately 100 volts. In this case, the net current to the collector plate is a function of the bias voltage and the electron velocity distribution function and is given by,

$$J_{net} = e\, n_i v_i - e \int_{\beta}^{\infty} v\, f_e(T_e, v)\, dv \qquad (5)$$

where,

$$\frac{1}{2} m_e \beta^2 = e V_o$$

and

$$f_e(v) = n_i [\frac{m_e}{2\pi k_b T_e}]^{1/2} \exp -[\frac{m_e v_i^2}{2 k_b T_e}].$$

The capacitive probe is shown in Figure 5 along with its model for analysis in Figure 6. The collecting surface was the outer conductror of a 0.086 inch diameter 50 Ω semi-rigid coax. A break in the outer conductor 3.8 cm from the end formed C_1 of the model. A 145 cm section of the coax was shielded from the beam and formed C_2. A series resistor and a section of 50 Ω coaxial transmission line made up the resistive divider. The values of C_1 and C_2 were chosen so they would charge up on a time scale short compared to a beam pulse with negligible current drain from the beam. The resistive divider was such that it could not appreciably discharge C_2 on the time scale of the beam.

The capacitive probe gave a measure of the beam floating potential, Φ_f, which is the potential at which the net current to the probe is zero. Assuming current is only collected on the upstream side of the probe, the ion velocity is known and the electron velocity distribution has been measured, the beam potential can be obtained from the floating potential using,

$$J_{net} = 0 = e\, n_i v_i - e \int_{\delta}^{\infty} v\, f_e(T_e, v)\, dv \qquad (6)$$

where,

$$\frac{1}{2} m_e \delta^2 = e\,(\Phi_b - \Phi_f)$$

Electron Velocity Distribution Measurements

To best duplicate the conditions used in the theoretical analysis of the neutralization process, two modifications were made to the diode. The cathode slots through which the beam was extracted were covered with a fine screen (50 x 50 strands/inch) to act as a dense localized source of axial electrons for neutralization. Secondly, the diode insulating magnetic field was prevented from reaching the beam extraction region by using flux excluders.

Biased charge collector measurements were made 0.5, 20, 30, and 41 cm from the diode. The peak collector current was measured for various bias voltages up to 1500 volts. Typical data and curves obtained from the theoretical analysis (6), (7) assuming a Maxwellian velocity distribution with three different values for the electron temperature ($v_{te}^2 = 2\,k_b T_e / m_e$) are shown in Figure 7. The theoretical curves show that the higher the electron thermal velocity, the higher the bias voltage required to stop the electrons on the tail of the distribution from reaching the collector plate. If the electron distribution consisted of cold electrons moving at the same velocity as the ions, the curve would be a step function at 196 volts (360 kV $\times m_e/m_i$).

The fit of the data points indicates that the electron velocity distribution is Maxwellian with a thermal velocity of approximately $0.9\, v_i$. As the bias voltage was increased, the number of electrons reaching the collector plate decreased and the net current increased. When the bias voltage was large enough (saturation region), all the electrons were stopped and only ion current was collected. The fact that the charge collector current levels off at high bias voltages indicates that secondaries emitted from the collector were not a significant factor.

The electron temperature was found to be independent of the distance from the diode indicating that the electrons were thermalized within 0.5 cm of the cathode. The large electron thermal velocity is consistent with the computer simulation predictions (4). The measured thermal velocity was found to be the same when the cathode screen was removed indicating that there was a sufficient number of electrons in the cathode plasma alone to neutralize the ion beam.

Floating Potential Measurements

It was impossible to measure the floating potential near the diode because of noise and because plasma from the diode gap formed an inductive connection between the probe and ground resulting in large amplitude LC oscillations. The onset and period of these LC oscillations increased in time as the probe was positioned farther from the diode confirming this interpretation. A transverse magnetic field between the probe and the diode was found to stop the oscillations by preventing current flow in this diode plasma channel.

In order to make the floating potential measurements the neutralization conditions were recreated downstream from the diode. The ion beam was neutralized and propagated through a metal bellows into a 7.6 cm diameter, 60 cm long Pyrex tube. A grounded conducting screen was placed at the entrance to the Pyrex tube to act as a dense, localized source of secondary electrons. A localized, transverse magnetic field was applied next to the screen in the bellows region (Figure 8). The magnetic field was produced by a permanent magnet with narrow pole pieces and was approximately 265 Gauss at the beam edge and 175 Gauss on axis. The magnetic field prevented the diode plasma from reaching the probe and could turn the neutralizing electrons while having negligible effect on the ions. This forced the ion beam to pick up a new set of neutralizing electrons from the grounded metal screen.

A typical capacitive probe signal is shown in Figure 9. The high frequency oscillations on the signal are due to reflections on the 145 cm section (C_2) of the probe. A graph of the floating potential at the peak of the beam pulse as a function of the distance from the screen is shown in Figure 10. The beam potential was found to be approximately 35 volts above the floating potential (Equation 6). The floating (beam) potential was found to drop from a value of 1431 (1466) volts at 0.3 cm from the screen to a value of 569 (604) volts approximatley 35 cm downstream of the screen.

The beam potential near the screen was close to the value of 1325 volts predicted by the computer simulations. The downstream beam potential was approximately three times higher than the predicted value of 196 volts and the thermalization distance was much longer than the predicted value of approximately 2 cm. The decrease of beam potential with distance is attributed to a thermalization of the neutralizing electrons. Since the beam potential is equal to the potential required to stop the electrons in the tail of the distribution from leaving the beam, the downstream potential indicates that when the electrons have thermalized the most energetic electrons have a velocity of approximately 2.8 v_i (Figure 11.).

A possible reason for the discrepancy in the thermalization distance and downstream potential could be the failure of the experiment to reproduce the conditions in the computer simulation or vice-versa. The non-localized transverse magnetic field may be a primary factor. Ideally, the transverse field should be infinitesimally thin in the direction of propagation. Electrons should be stripped from the beam and replaced by secondaries from the screen over a short distance. In reality the transverse field was not localized and the position where the transverse field tried to strip off the electrons did not coincide exactly with the location of the source of secondary electrons. This could result in a new set of neutralizing electrons whose initial distribution was already somewhat thermalized, producing a weaker two-stream instability than predicted by the simulation.

The floating potential at the screen was measured for various values of ion velocity by varing the diode voltage. The beam potential normalized to,

$$\frac{1}{2}\frac{m_e(2.7\,v_i)^2}{e} \qquad (7)$$

is plotted as a function of the diode voltage in Figure 12. Over the range of ion velocities studied the potential scaled with v_i^2 as predicted by the computer simulation.

Conclusions

Experimental observations of an intense, pulsed ion beam neutralized by a dense localized source of electrons reveal that the downstream electron velocity distribution is Maxwellian with a thermal velocity of approximately $0.9\,v_i$. The thermalization of the electrons occurred within 0.5 cm of the diode indicating a rapid thermalization mechanism. When the neutralizing electrons were removed from the beam by a transverse magnetic field and replaced by secondaries, the floating and beam potentials were found to decrease with distance from the secondary source as the new neutralizing electrons thermalized. These observations are consistent with existing electrostatic ion beam neutralization theories (3), (4), (5).

References

1. J. A. Nation, Particle Accelerators, 10, 1 (1979).

2. S. Humphries, Jr., Nuclear Fusion, 20, 1549 (1980).

3. S. Humphries, Jr., App. Phys. Lett., 32, 792 (1978).

4. S. Humphries, Jr., T. R. Lockner, J. W. Poukey and J. P. Quintenz, Phys. Rev. Lett., 46, 995 (1981).

5. R. N. Sudan, Appl. Phys. Lett., 44, 957 (1984).

6. R. Kraft, PhD. Thesis, Cornell University (1985).

7. R. Kraft and B. R. Kusse, Laboratory of Plasma Studies Report No. 358, Cornell University (1986).

Figure Captions

Figure 1. Magnetically insulated diode.

Figure 2. Ion beam parameters: a) Inductively corrected voltage; b) Diode current; c) Ion current density.

Figure 3. Beam profiles: a) Beam potential vs. position; b) Ion and electron density vs. position; c) Ion and electron velocity distributions.

Figure 4. Electron distributions: a) Electron phase space plots at two times; b) Downstream electron velocity distributions corresponding to regions indicated in phase space plot. Humphries, S., Jr., et al., Phys. Rev. Lett., 46 995 (1981).

Figure 5. Capacitive probe.

Figure 6. Capacitive probe model.

Figure 7. Theoretical biased charge collector curves for for three different electron thermal velocities and experimental data 20 cm from the diode.

Figure 8. Transverse magnetic field and neutralizing screen.

Figure 9. Typical capacitive probe signal.

Figure 10. Floating potential vs. distance from screen.

Figure 11. Electron velocity distribution inferred from the biased charge collector and capacitive probe data.

Figure 12. Normalized floating potential as a function of the diode voltage.

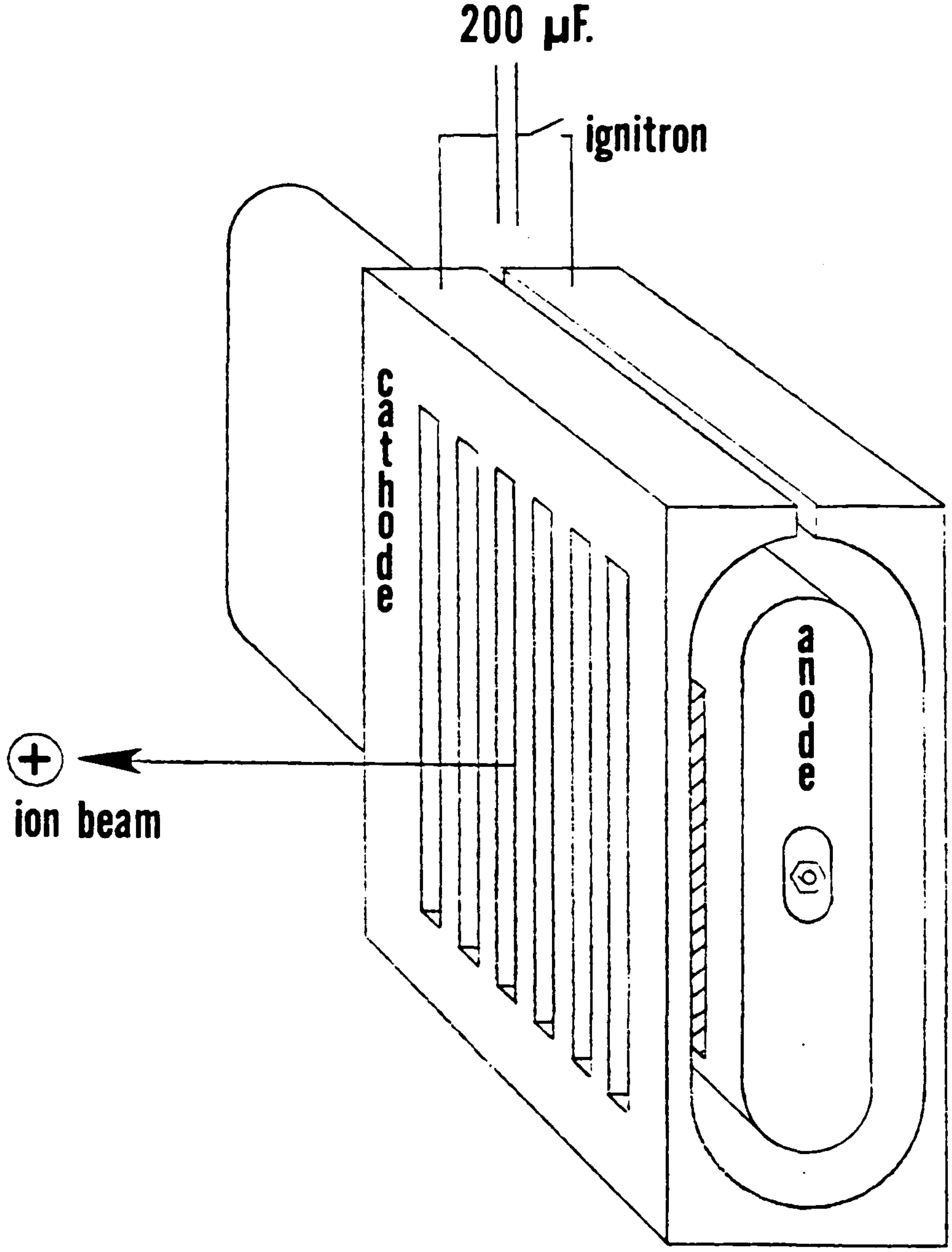
200 μF.
ignitron
cathode
anode
ion beam

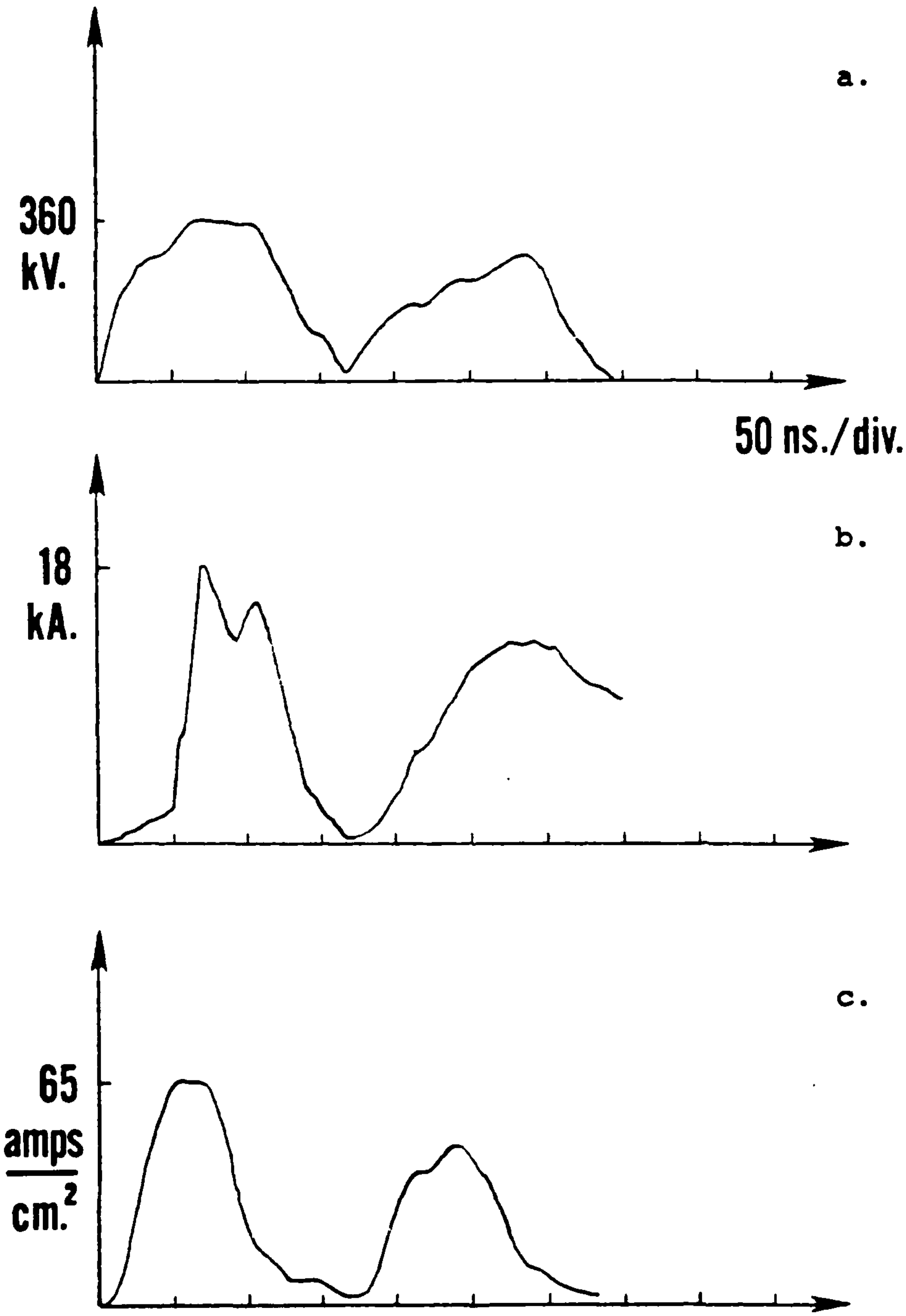
a.
360
kV.
50 ns./div.
b.
18
kA.
c.
65
amps
cm.²

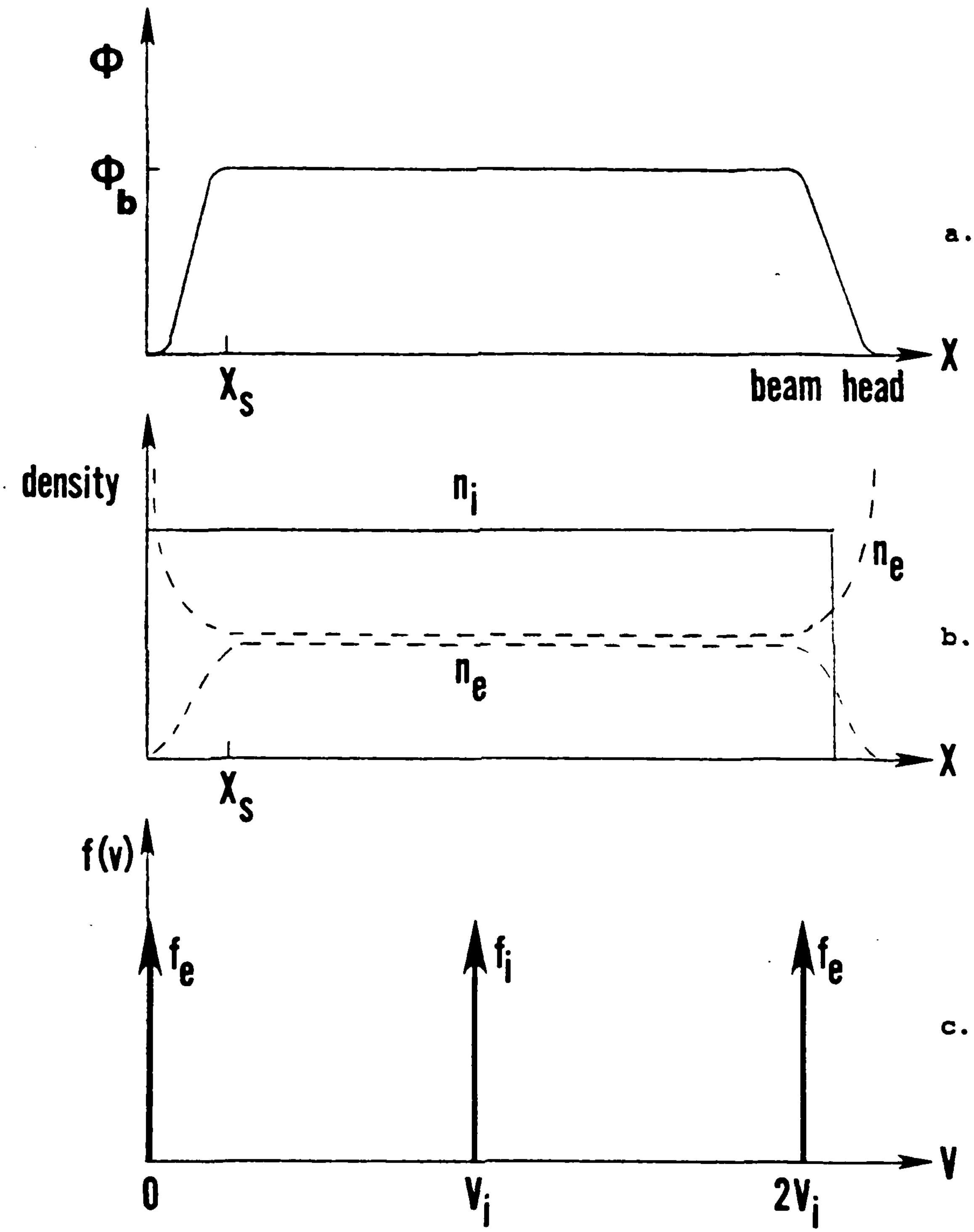

Φ
Φ_b
a.
X
X_s
beam head
density
n_i
n_e
b.
n_e
X
X_s
f(v)
f_e
f_i
f_e
c.
V
0
V_i
$2V_i$

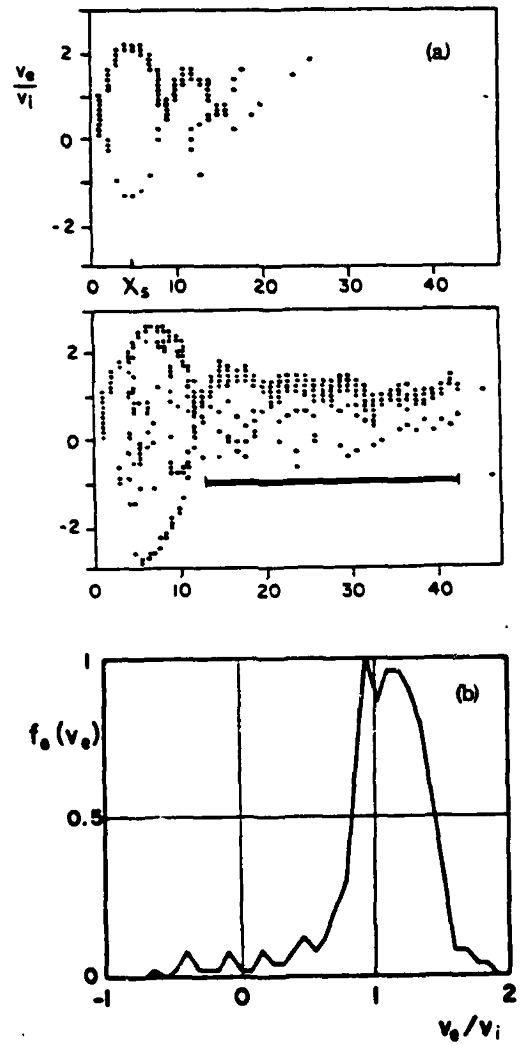

(a)
v_e/v_i
2
0
-2
0
X_s
10
20
30
40
(b)
$f_e(v_e)$
1
0.5
0
-1
2
v_e/v_i

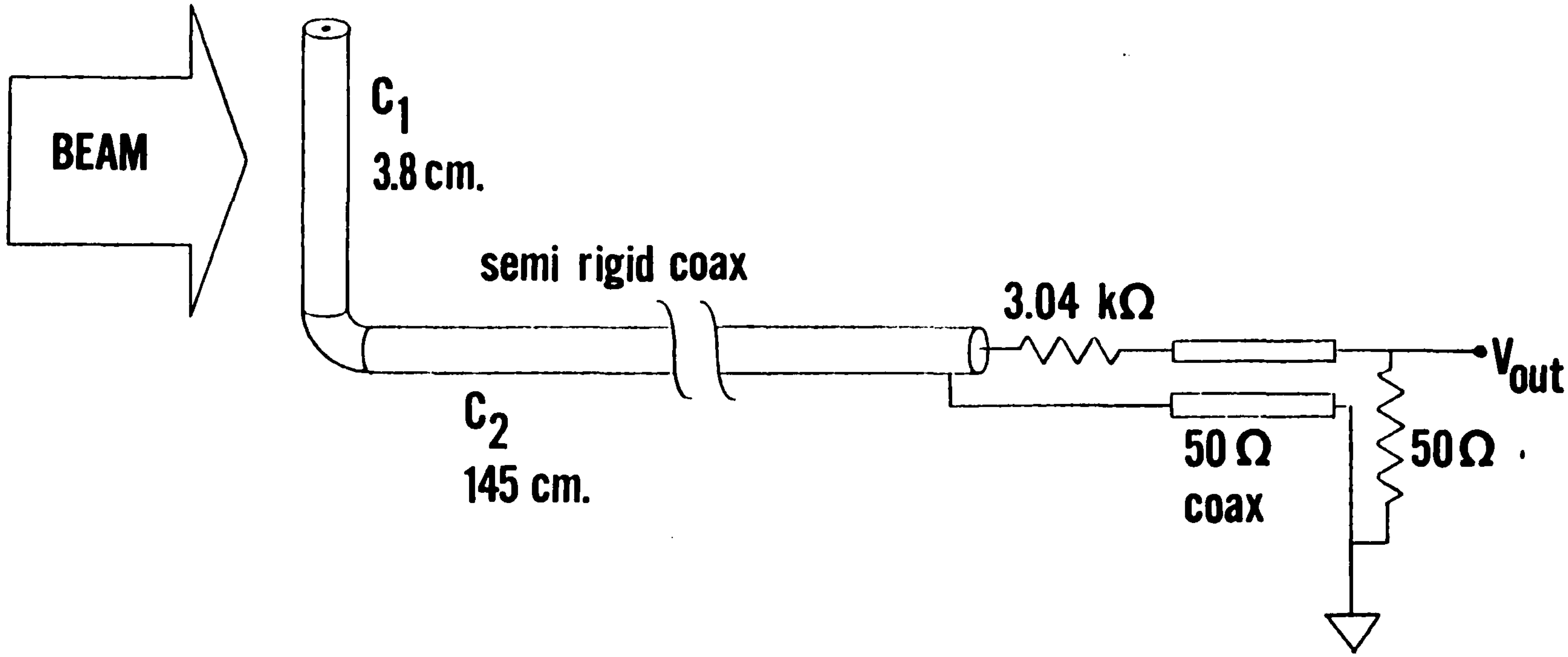
BEAM
C1
3.8 cm.
semi rigid coax
C2
145 cm.
3.04 kΩ
50 Ω
coax
50 Ω
Vout

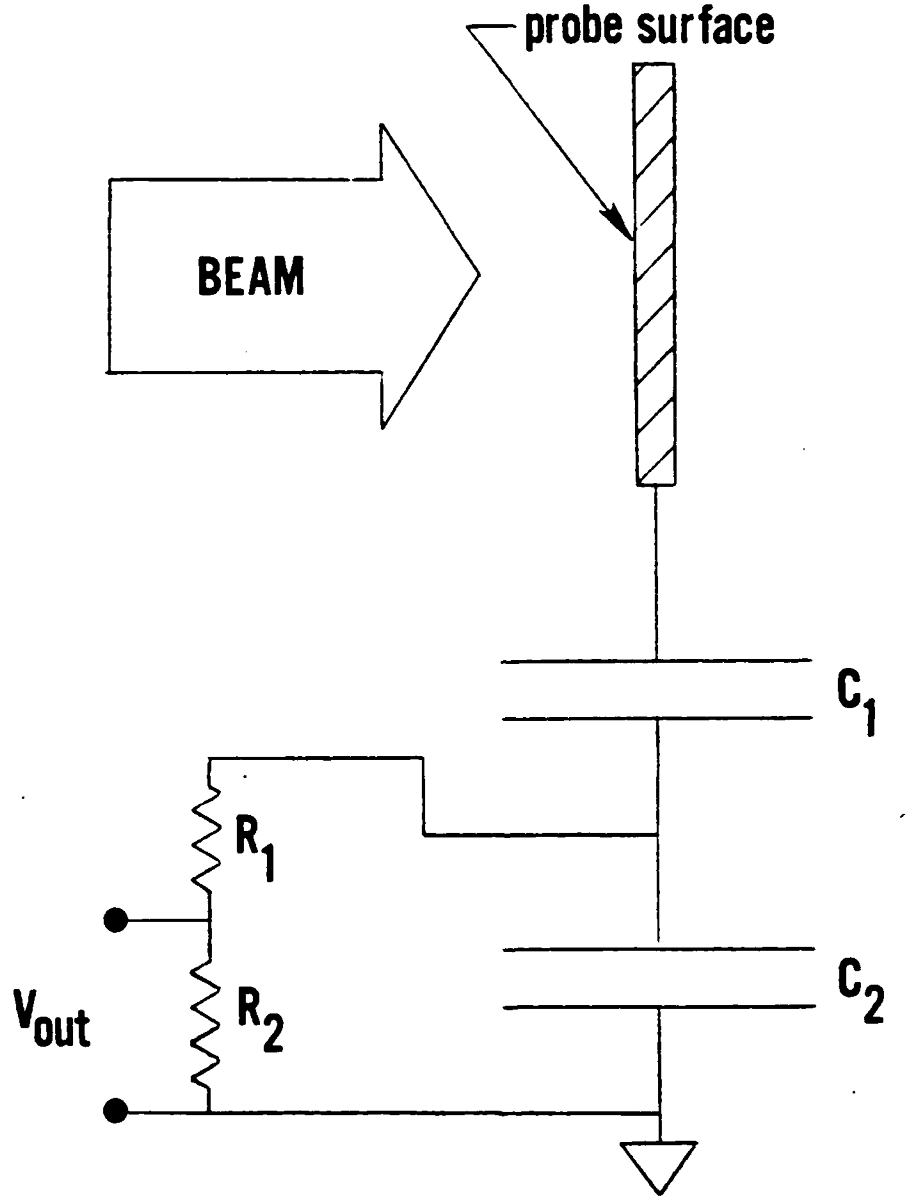
probe surface
BEAM
C1
R1
C2
Vout
R2

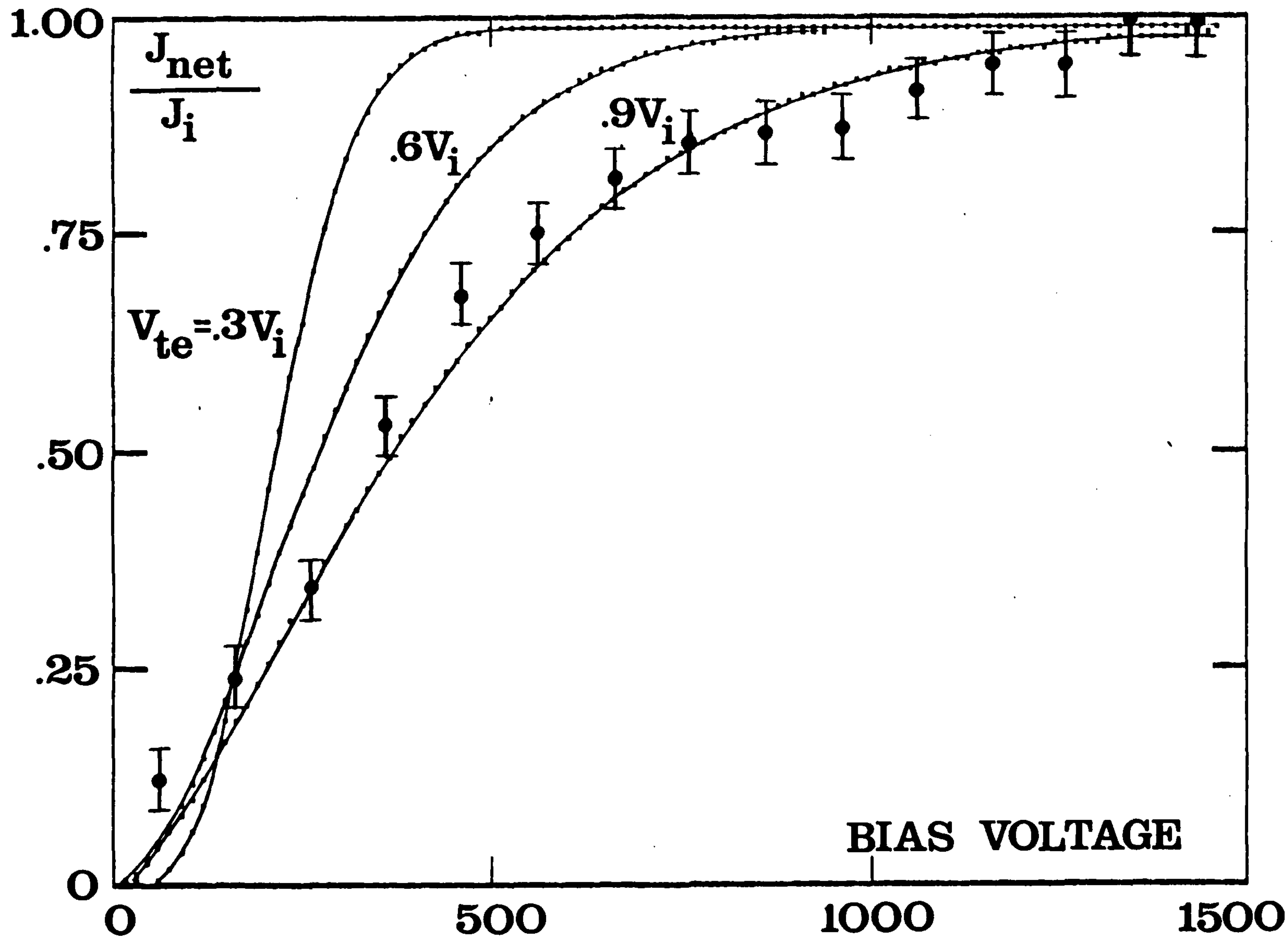
1.00
.75
.50
.25
0
Jnet / Ji
Vte=.3Vi
.6Vi
.9Vi
0
500
1000
1500
BIAS VOLTAGE

8

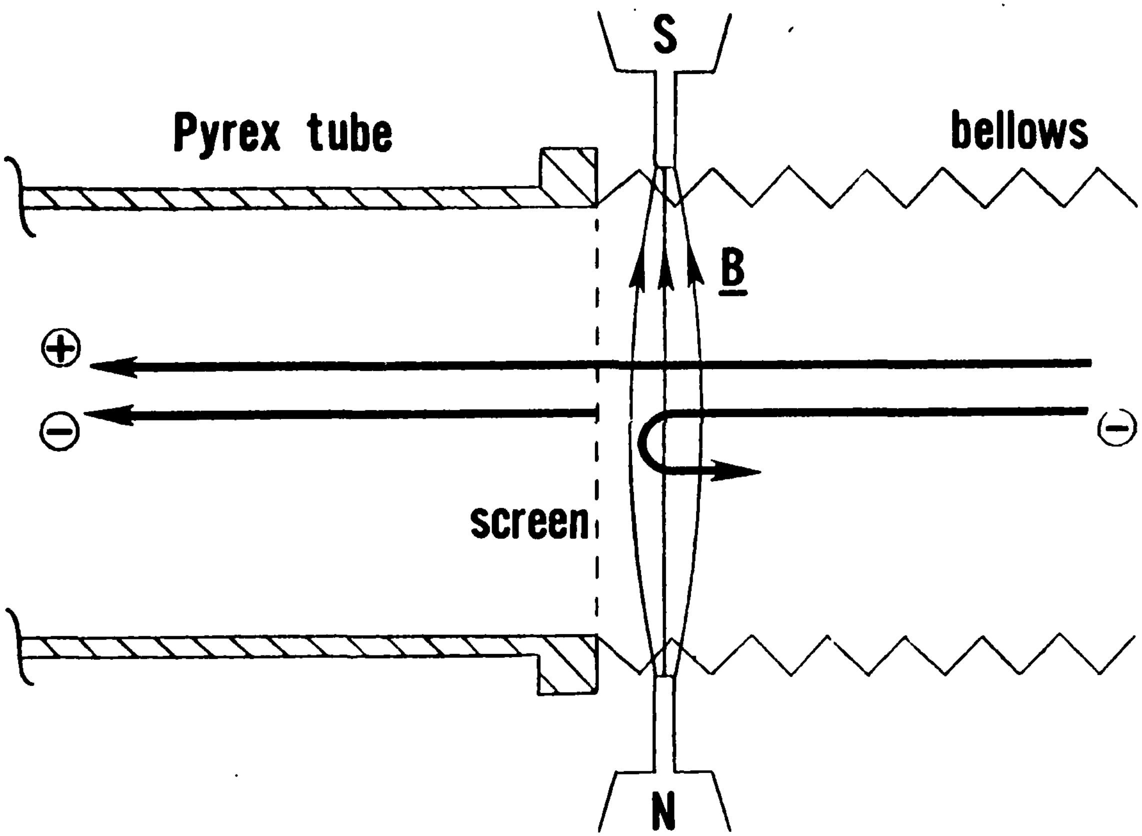

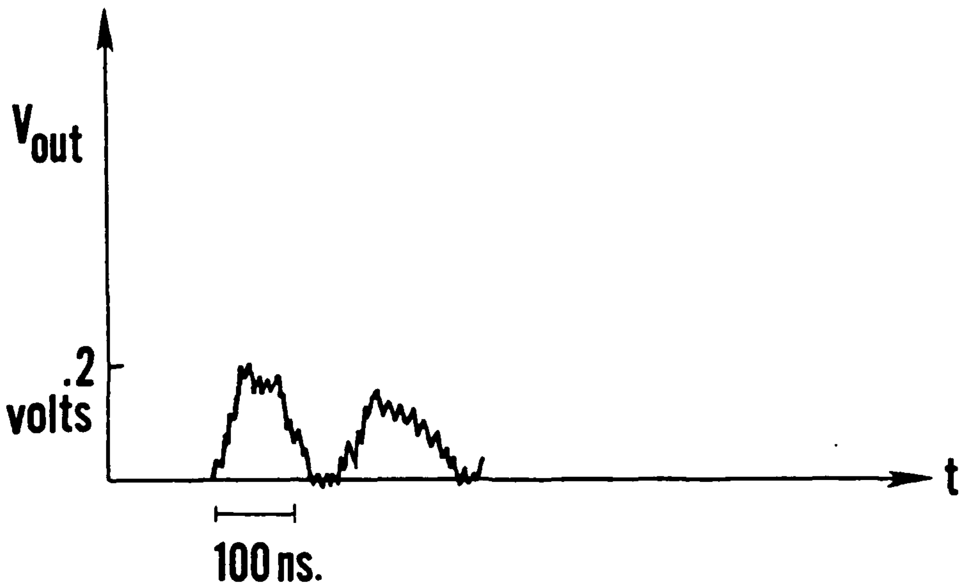

V_{out}
.2
volts
t
100 ns.

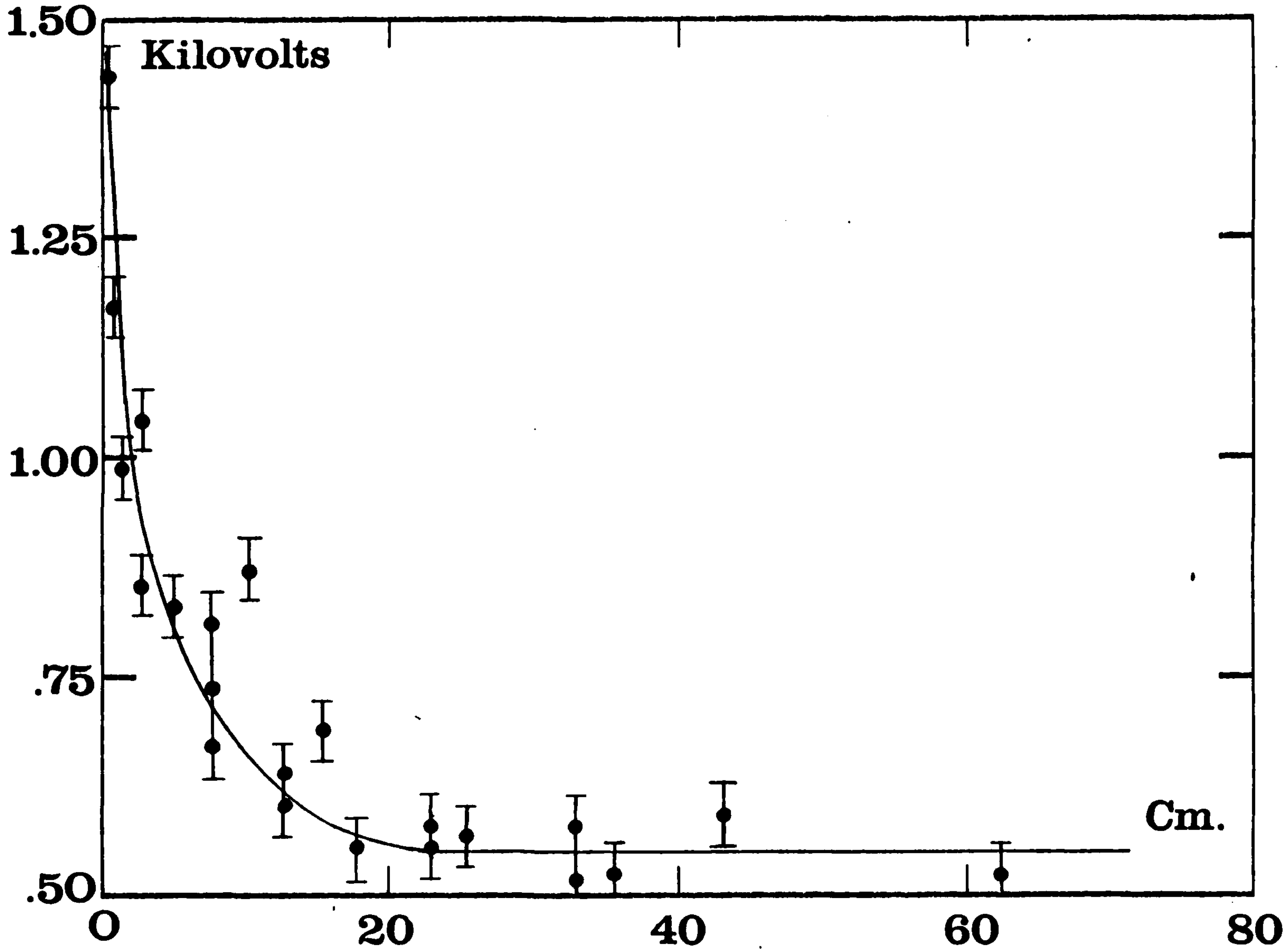
Kilovolts
1.50
1.25
1.00
.75
.50
0
20
40
60
80
Cm.

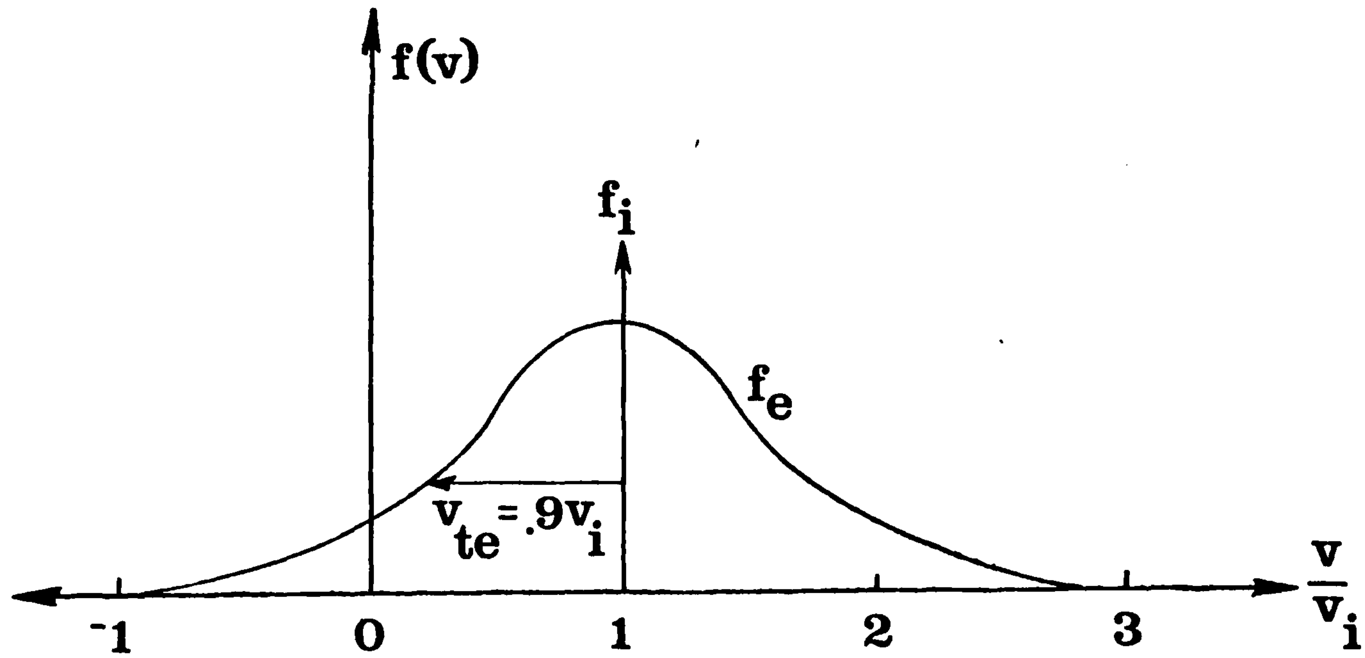

f(v)
f_i
f_e
v_te = .9v_i
-1
0
1
2
3
v/v_i

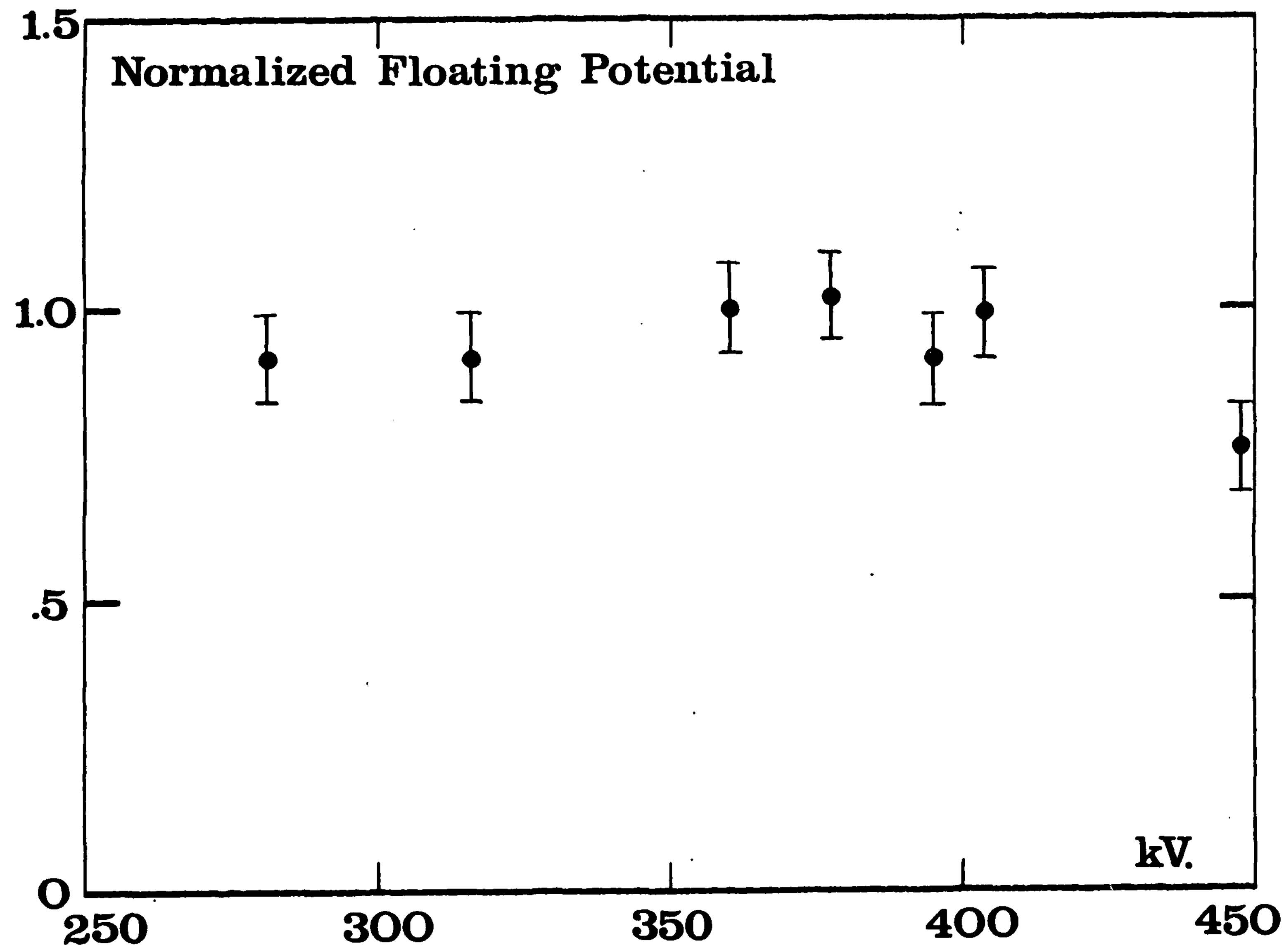
Normalized Floating Potential
1.5
1.0
.5
0
250
300
350
400
450
kV.